Topics in Catalysis (2023) 66:1440–1450
https://doi.org/10.1007/s11244-023-01792-w

ORIGINAL PAPER

Influence of Support Structure on Catalytic Performance of Supported Liquid-Phase (SLP) Catalysts in Hydroformylation of 1-Butene

Mahtab Madani[1] · Leonhard Schill[1] · Nanette Zahrtmann[2] · Raquel Portela[3] · Linda Arsenjuk[4] · Robert Franke[4] · Rasmus Fehrmann[1] · Anders Riisager[1]

Accepted: 16 February 2023 / Published online: 6 March 2023

Abstract

Several supported liquid-phase (SLP) catalysts with immobilized Rh-biphephos complexes on monolithic supports were prepared and applied for continuous gas-phase hydroformylation (HyFo) of 1-butene. The support comprised macroporous monolithic silicon carbide (SiC) with deposited silica nanoparticles (NPs) in order to provide mesopores with enhanced capillary forces to retain the liquid-phase. Variable parameters were examined for the monolithic SiC supports, including size and loading of deposited silica NPs and intermediate calcination between silica deposition steps to obtain the most efficient support configuration for the SLP system. The SLP catalysts with larger deposited silica NPs gave higher catalytic activity (i.e. 1-butene conversion and turnover frequency) compared to the supports with smaller sized silica NPs. However, the selectivity towards the preferred linear aldehyde was higher in the SLP catalysts with supports containing less silica with small silica NPs. Importantly, the prepared SLP catalyst systems showed long-term stability in HyFo with negligible formation of high boiling aldol condensation products.

Keywords SLP catalyst · Hydroformylation · Heterogenization · Silicon carbide · Monolith · Porosity

1 Introduction

Homogeneous catalysis with dissolved metal complexes typically offers several advantages compared to its heterogeneous counterpart such as high activity and selectivity. However, the challenging separation of the metal complexes from the liquid reaction mixture hampers the large-scale industrial implementation of many promising catalysts [1–3]. Several strategies have been proposed and implemented to overcome this drawback, including heterogenization of the homogeneous catalysts, which facilitates the product separation and complete catalyst recovery while maintaining the activity and selectivity of the catalyst [4–6]. Supported liquid-phase (SLP) catalyst systems comprise examples of such a heterogenization strategy, where the catalytic compounds are dissolved in a liquid-phase and dispersed on the surface of a high-surface-area, porous solid support material [7–10]. This makes the resulting SLP system heterogeneous-like at macroscopic scale, while its microscopic function resembles a homogeneous catalyst [11].

SLP catalysts, including those based on supported ionic liquid-phase (SILP), have been used in fixed-bed reactors with impregnated support grains for numerous reactions, including hydroformylation (HyFo) [12–16]. In the HyFo reaction, olefins are converted into either linear (n-) or branched (iso-) aldehydes in the presence of syngas (CO/H_2 gas mixture) by a transition metal complex catalyst (Scheme 1). HyFo is a highly important industrial application of homogeneous catalysis [17] with an annual aldehyde production of more than 9 million tons (2017) [18]. Industrial HyFo catalysts are based mainly on Co- or Rh-complexes with Rh-based processes operating at much milder conditions (temperature and pressure) [17]. The

✉ Anders Riisager
ar@kemi.dtu.dk

1 Centre for Catalysis and Sustainable Chemistry, Department of Chemistry, Technical University of Denmark, Kemitorvet Building 207, 2800 Kgs, Lyngby, Denmark

2 LiqTech Ceramics A/S, Industriparken 22C, 2750 Ballerup, Denmark

3 Institute of Catalysis and Petrochemistry (ICP-CSIC), Spectroscopy and Industrial Catalysis Group, C/ Marie Curie, nº2.Cantoblanco, Madrid, Spain

4 Evonik Operations GmbH, Paul-Baumann-Str. 1, 45772 Marl, Germany

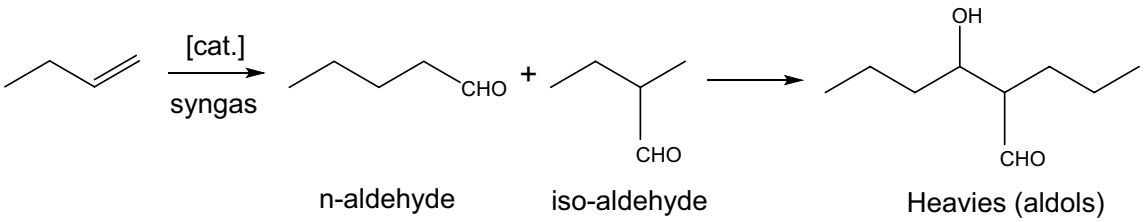

Scheme 1 Hydroformylation of 1-butene to linear and branched aldehydes with the undesired consecutive aldol condensation reaction leading to the formation of 3-hydroxy-2-propylheptanal

ligand inventory is important as it influences the catalyst regioselectivity towards n- or iso-aldehyde product formation, which is commonly expressed as either the molar n/iso ratio or as the percentage share of the linear product.

The primary aldehyde products formed in the HyFo reaction are key building blocks for the chemical industry as intermediates for the production of a large variety of derived bulk chemicals such as alcohols, carboxylic acids, and amines [17]. However, the aldehyde products can also partake in an exothermic aldol condensation reaction and form heavier molecules (high-boiling aldol condensation products like 3-hydroxy-2-propylheptanal), which are typically undesired as they accumulate in the system hampering the catalytic activity over time [19]. SILP catalysts have shown to be prone to catalyst deactivation caused by accumulation of aldehyde products and high boilers in the ionic liquid, thus making its industrial application challenging [20, 21]. This accumulation can be suppressed when bis(2,2,6,6-tetramethyl-4-piperidyl)sebacate (abbreviated as sebacate; Fig. 1) is used as an alternative liquid phase [22], where lower reactant/product solubility compared to ionic liquids makes aldol formation and condensation less pronounced [23]. Notably, sebacate melts at 82–85 °C and forms therefore a liquid-phase at HyFo reaction temperatures that are typically ≥ 90 °C. Additionally, due to its two basic moieties the molecule can act as an acid scavenger [24], slowing down autocatalytic ligand decomposition.

Upscaling of grained-sized SLP catalyst systems may be challenging due to insufficient heat transfer and large pressure drop over the catalyst bed [25, 26]. Monolithic silicon carbide (SiC) supports are promising alternatives to fixed-bed reactors with grains due to important advantages such as, e.g. efficient thermal conductivity, chemical inertness [27] and low pressure drop. Their modular design makes them also suitable for simple upscaling [28]. In SiC monolith SLP systems, the required mesoporosity to confine the liquid-phase inside the porous structure through capillary forces can be generated by deposition of nanometer sized metal oxides (e.g., SiO_2) into the macropores. In addition, the monolithic supports can be coated by polymeric membranes to have potential applications for *in-situ* product separation by membrane reactor systems. For this purpose, a relatively smooth macroporous skin can be applied on the outer surface of the SiC monolith using sub-micrometer sized SiC particles [29].

In this work, several SLP catalysts were prepared from $Rh(acac)(CO)_2$ precursor, diphosphite ligand biphephos (bpp), and the additive bis(2,2,6,6-tetramethyl-4-piperidyl) sebacate (Fig. 1) with membrane-less SiC monoliths as the support. The structural properties of the monolithic supports were tuned by washcoating with silica nanoparticles (NPs), and the catalytic performance of the resulting SLP catalysts evaluated for gas-phase HyFo of 1-butene to establish structure-performance correlations and verify long-term stability of the catalysts.

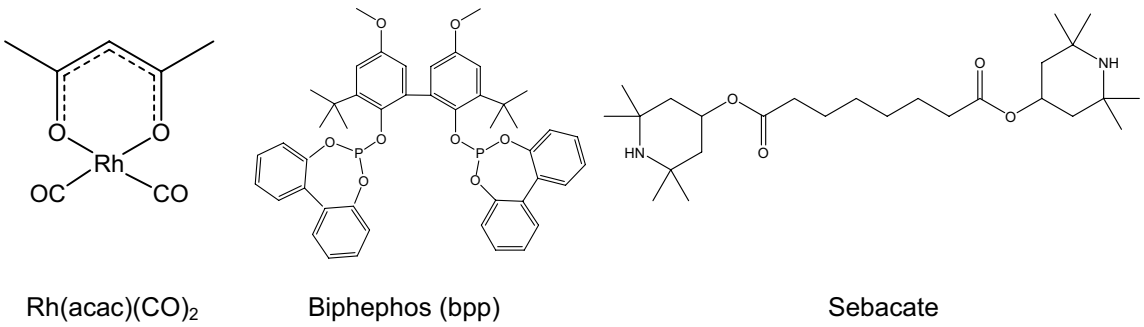

Fig. 1 The components of the catalytic systems examined for gas-phase HyFo of 1-butene

2 Experimental

2.1 Preparation of SiO_2/SiC Monolithic Supports

SiC monoliths were manufactured by LiqTech Ceramics A/S (Fig. 2) following a patented procedure [30]. According to the previously published work [23], a polymeric formulation of α-SiC powder was shaped into a multi-channel monolith by extrusion, which was then dried and sintered at an appropriate temperature (SiC core). A suspension of sub-micrometer sized α-SiC particles was subsequently applied onto the surface of the monolith, which was then dried and sintered to form the SiC skin [31]. The monoliths measured 200 mm × 25.4 mm and contained 30 channels of 3 mm diameter.

To modify the monoliths with mesoporosity, a washcoat with SiO_2 NPs (7 or 70 nm) was applied by submerging the SiC body into a colloidal suspension. Afterwards, excess liquid was removed by gravity followed by drying overnight at room temperature, and calcination at standard temperature in the range of 500–700 °C [31] with a ramp of 100 °C h^{-1} and a minimum hold time of 1 h. The variations in the prepared SiO_2/SiC monolithic supports are summarized in Table 1.

2.2 Characterization of SiO_2/SiC Monolithic Supports

The textural properties of the supports were determined by mercury intrusion porosimetry (MIP) in a CE Instruments Pascal 140/240 mercury intrusion porosimeter after predrying of the samples overnight at 150 °C. The calculation of pore diameters was based on the Washburn equation [32] assuming a non-intersecting cylindrical pore model. The mercury contact angle of 141° and surface tension of 484 mN m^{-1} were used as recommended by IUPAC. The change from low to high pressure took place at 30 psi corresponding to 7.3 µm, thus possibly creating artifacts at 6–8 µm.

Table 1 Overview of the prepared SiO_2/SiC monolithic supports

Support name	SiO_2 NP size (nm)	Number of SiO_2 washcoat layers	Intermediate calcination between SiO_2 washcoat layers
1 × Si 7	7	1	No
1 × Si 70	70	1	No
2 × Si 70	70	2	No
2 × Si 70-calc	70	2	Yes

Brunauer–Emmett–Teller (BET) analysis of selected supports was further performed at liquid nitrogen temperature (− 196 °C) using a Micromeritics ASAP 2020 instrument. Prior to the analysis samples were outgassed at 300 °C for 3 h.

Scanning electron microscopy (SEM) images and energy-dispersive X-ray (EDX) mapping of the different monolithic supports were recorded using an FEI Quanta FEG 250 ESEM microscope operated at 15 kV, with the working distance of 5.0 mm.

^{29}Si solid-state magic angle spinning nuclear magnetic resonance (MAS NMR) spectra of supports were recorded on a Bruker AVANCE III HD spectrometer operating at a magnetic field of 14.05 T equipped with a 4 mm CP/MAS BBFO probe. The spectra were acquired using a 4.75 ms p/2 excitation pulse and an interscan delay of 45 s. High-power SPINAL64 ^{1}H decoupling was applied during acquisition. The chemical shifts are reported relative to tetramethylsilane (TMS; 0 ppm).

2.3 Preparation of SLP Catalysts Using SiO_2/SiC Monolithic Supports

The different SLP catalyst systems were prepared by immobilization of a Rh/bpp/sebacate catalyst stock solution on the four different SiO_2/SiC monolithic supports using the

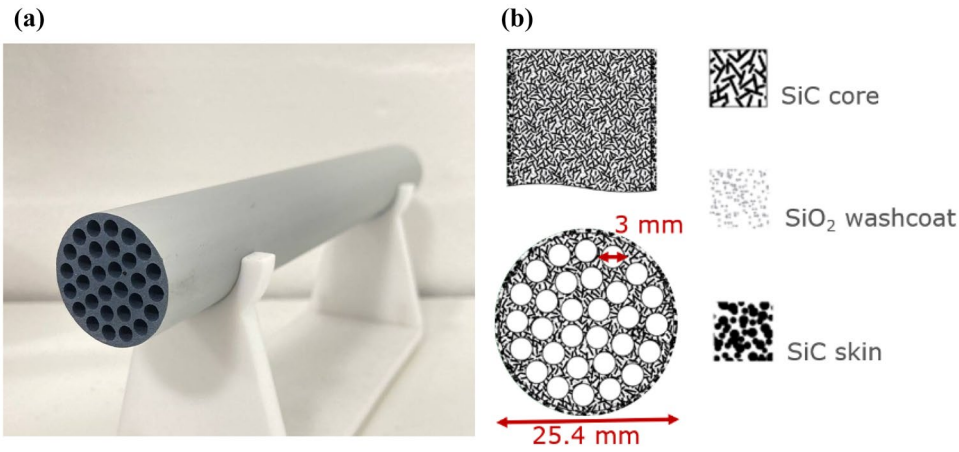

Fig. 2 **a** Picture of membraneless SiC monolith support and **b** schematic drawing of the SiC monolithic support with mesoporosity generated by deposition of SiO_2 NPs

procedures described below. All chemicals were used as received from the suppliers.

2.3.1 Preparation of Catalyst Stock Solution

0.6268 g (0.79 mmol) of ligand (6,6′-[(3,3′-di-tert-butyl-5,5′-dimethoxy-1,1′-biphenyl-2,2′-diyl)bis(oxy)]-bis(dibenzo[d,f][1–3]-dioxaphosphepin (biphephos or bpp, > 98%, Evonik Oxeno GmbH), 0.0514 g (0.19 mmol) of Rh-precursor dicarbonyl(acetylacetonato)rhodium(I) (Rh(acac)$(CO)_2$, > 98%, Sigma-Aldrich), and 1.533 g (3.18 mmol) of additive bis(2,2,6,6-tetramethyl-4-piperidyl)sebacate (sebacate, > 98%, Evonik Oxeno GmbH) corresponding to a molar ratio of Rh/bpp/sebacate of 1/4/16 were dissolved in 30 mL anhydrous CH_2Cl_2 (≥ 99.8%, Sigma-Aldrich) under an argon atmosphere (99.999%) using standard Schlenk technique.

2.3.2 Impregnation of SiO_2/SiC Monolithic Supports

The SiO_2/SiC monoliths were before impregnation dried in an oven at 100 °C overnight, and then treated under vacuum for a minimum of 4 h. The monolithic supports were stored in a vertical position and impregnated with the prepared catalyst stock solution by dropwise addition of the solution to the top end of the monoliths' cross-section under an argon atmosphere using a Schlenk system (Figs. S1 and S2 in the supporting information). The excess solution was drained and the monoliths dried at room temperature with an argon flow for about 2 h and subsequently under vacuum until a constant weight was obtained (typically 4 h). The content of Rh metal in the monoliths was determined by the weight increase after impregnation assuming a homogeneous stock solution and total evaporation of the solvent. Accordingly, monolithic SLP catalysts with 1 × Si 7, 1 × Si 70, 2 × Si 70, and 2 × Si 70-calc. contained 12.70, 12.05, 10.11, and 9.74 mg Rh, respectively, corresponding to 0.012, 0.011, 0.009, and 0.008 wt% Rh.

2.4 Gas-Phase Hydroformylation of 1-Butene Using SLP Catalyst Systems

The catalytic performance tests of the monolithic SLP catalysts for continuous gas-phase HyFo of 1-butene were carried out in a customized reactor set-up in retentate mode (Fig. S3, detailed flowsheet of the reactor set-up depicted in Fig. S4) for 140 h time on stream (TOS) with a feed containing 1-butene (99.5%), carbon monoxide (99.97%), hydrogen (99.999%), and nitrogen (99.999%). The reactor was assembled inside a glovebox and mounted in the set-up with nitrogen flow of 1000 mL min^{-1} to prevent possible air contamination. After mounting, the reaction temperature was set to 120 °C with absolute feed pressure of 10 bar using a start-up procedure where the feed components were gradually increased in order to limit aldol formation and to make the reaction smoother [33]. The gas-flow rates were regulated by mass-flow controllers (MKS, GM50A), while 1-butene flow was dosed using an HPLC Smartline pump 100 (Knauer) equipped with a 10 mL pump head. The feed flow rates used during the catalytic performance testing are summarized in Table 2.

The outlet gas composition was analyzed by on-line gas chromatography (Agilent 7890 A gas chromatogram). The organic compounds were separated by a DB-1 by J&W Scientific column (50 m × 0.320 mm × 5.00 µm) and detected by a flame ionization detector (FID). The kinetic evaluation of catalytic experiments (calculations of conversion, selectivity, and turnover frequency) can be found in the supporting information (Eqs. S1-S4).

3 Results and Discussion

3.1 Support Properties

The monolithic supports were prepared with silica washcoat variations based on commercially available 7 and 70 nm silica particles (Table 1). Silica NPs larger than 70 nm were not used as such particles would generate larger interparticle mesopores and weaker capillary forces, thus making the resulting catalysts more prone to leaching of the liquid phase under operating conditions. Furthermore, larger mesopores will create less surface area resulting in a thicker liquid film, which can potentially cause transport limitations and promote aldol formation due to a longer residence time of the produced aldehydes in the liquid phase.

The morphology of the SiC monolithic materials was analyzed by SEM. Figure 3a shows the morphology of the SiC core (the lower part), and the smooth surface of the SiC skin (the upper part) made by sub-micrometer sized SiC particles. Figure 3b and c show the SiC particles in the core

Table 2 Gas flow rates during time on stream of gas-phase HyFo of 1-butene using SLP catalysts

Time on stream (h)	CO (mmol min^{-1})	H_2 (mmol min^{-1})	1-butene (mmol min^{-1})	N_2 (mmol min^{-1})
0–22	1.56	1.56	0.36	12.19
22–44	3.13	3.13	0.73	8.66
44–140	4.46	4.46	1.04	5.67

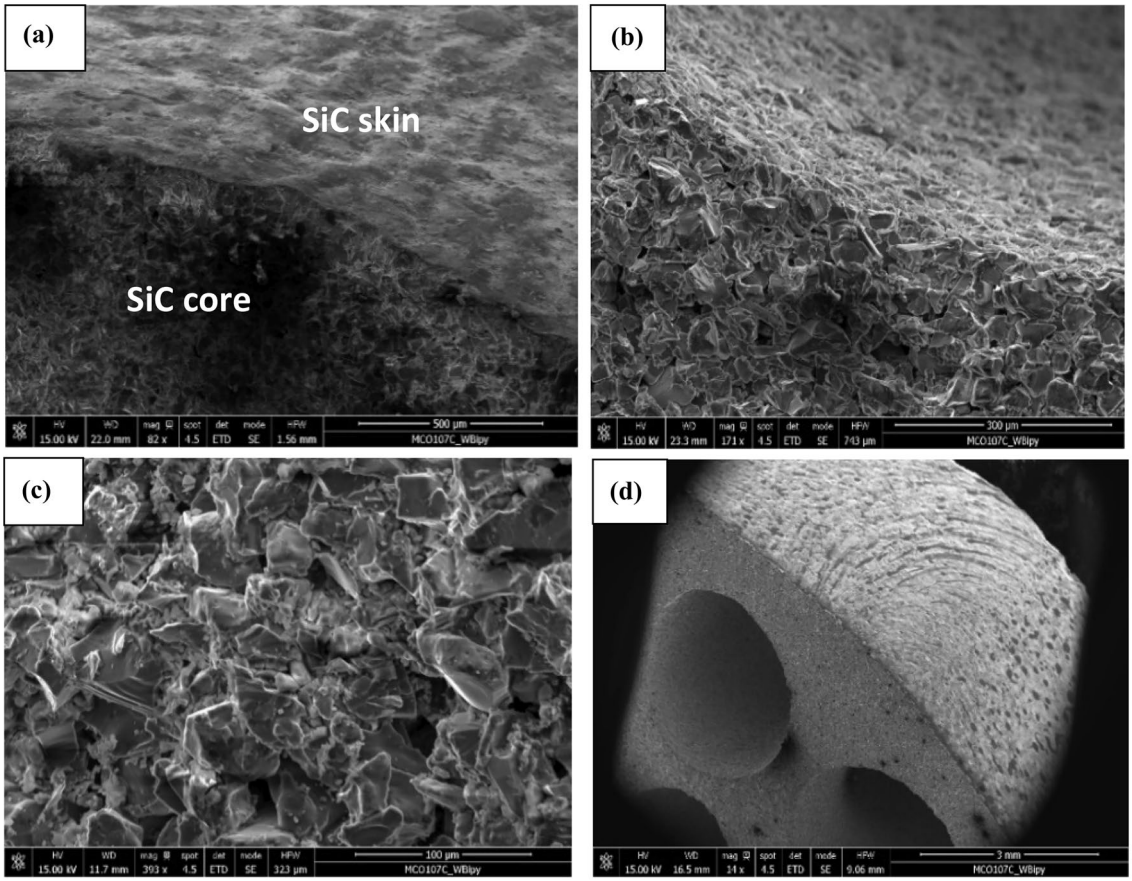

Fig. 3 SEM images of SiO_2 washcoated SiC monolithic support with focus on **a** SiC core and skin, **b** and **c** SiC core structure and **d** SiC skin and core with the view of the monolith's channels

support with porosity generated by interparticle voids of the SiC particles having diameters between 9 and 55 µm (mean particle size 30 µm), determined by line measurement. A histogram of the SiC particle size distribution in the SiC core support is included in Fig. S5. Notably, EDX mapping of the 1 × Si 7, 1 × Si 70, 2 × Si 70 core supports showed a homogeneous distribution of the SiO_2 NPs in the SiC pore structures (Figs. S6-S9).

MIP results of the pristine SiC monolith with SiC skin have previously [23] shown a macroporous structure with a bimodal size distribution comprising a low volume of macropores smaller than 1 µm related to the skin, and mostly large macropores belonging to the interparticle voids between the core SiC particles with diameter of several µm depending on the SiC particle size. To reduce the pore size and increase the pore area SiO_2 NPs with sizes of 7 or 70 nm were deposited in the SiC monolith supports followed by calcination at a moderate temperature (below 700 °C) to avoid silica sintering. Such support modification generates mesopores with improved catalyst immobilization capability via capillary forces, which potentially avoids leaching of the liquid catalyst phase during catalysis [34].

Analysis by MIP (Fig. 4) confirmed that the deposited SiO_2 NPs partially filled the macrovoids between the SiC particles in the monoliths. This resulted in a trimodal pore size distribution related to unfilled large macropores, newly generated small macropores, and mesopores between the SiO_2 NPs. The small macropores were likely formed by accumulation of the SiO_2 NPs into original macropores, which resulted in a reduction of the neck size of the pores. The size of the newly generated mesopores by the 70 nm SiO_2 NPs were around 22 nm in diameter, while no mesopores were detected in the support with 7 nm SiO_2 NPs by this technique (Fig. 4a). The latter result could arise due to the low SiO_2 loading, the small voids between the 7 nm particles, and because the smaller SiO_2 particles were prone to sintering at the specific calcination temperature [23]. Moreover, pores smaller than 3 nm are not detectable by MIP as they are below the detection limit.

For the monoliths with lower SiO_2 loading (1 × Si 7 and 1 × Si 70) the volume of the large macropores (interstitial voids between SiC particles) was larger (Fig. 4b). The MIP results revealed total pore areas for each support variation 1 × Si 7, 1 × Si 70, 2 × Si 70, and 2 × Si 70-calc. of 0.2, 3.6,

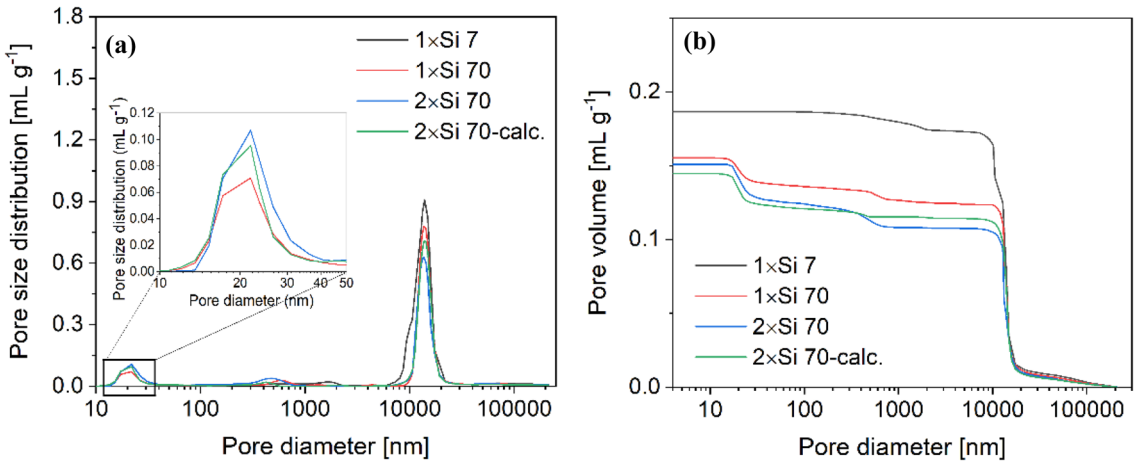

Fig. 4 **a** Pore size distribution with the magnification in mesopores region, and **b** cumulated pore volume of the SiC monoliths with various loadings of deposited SiO_2 NPs

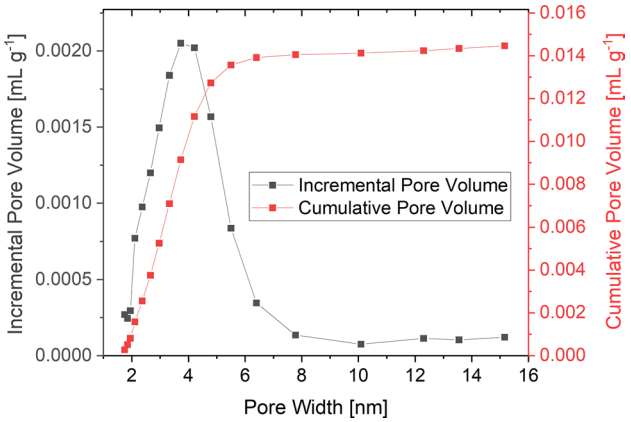

Fig. 5 Pore size distribution and pore volume data of the 1 × Si 7 support derived from N_2-physisorption

4.9, and 4.5 $m^2\ g^{-1}$, respectively. Thus, by increasing the size and amount of mesopores in the SiC supports, the total pore area also increased.

As MIP was not successful in detecting the presence of small mesopores in 1 × Si 7, N_2-physisorption analysis was performed to evaluate the existing mesopores in this support. As depicted in Fig. 5, the monomodal pore size distribution was centered at 3.7 nm and the corresponding BET surface area was 18.7 $m^2\ g^{-1}$, showing that the 7 nm sized silica particles did not sinter at the employed calcination temperature.

3.2 Gas-Phase Hydroformylation of 1-Butene

The SLP catalysts were prepared by immobilization of a catalyst stock solution with a Rh/bpp/sebacate molar ratio of 1/4/16, as this specific ratio was found in previous studies to result in good catalyst performance [29, 35]. The excess of sebacate is required as acid scavenger in the system, whereas the Rh/bpp ratio of 1/4 is lower than the usual ratio of 1/10 reported for related SILP catalyst systems [6]. The reduced content of expensive bpp ligand lowers the catalyst cost, which is important for the possible large-scale industrial implementation.

The continuous gas-phase HyFo of 1-butene with a first series of prepared SLP catalysts with different modifications resulted in 1-butene conversions and TOF values as presented in Fig. 6, and a second series of analogous catalysts yielded similar results thus confirming good reproducibility of the systems (Figs. S10-11). The catalysts with supports having one- and two-layers of 70 nm SiO_2 NPs showed the best catalytic activities comprising semi-steady state 1-butene conversion of ca. 80% corresponding to a $TOF_{1\text{-butene}}$ around 500 $mol_{1\text{-butene}}\ mol_{Rh}^{-1}\ h^{-1}$. Notably, these catalysts yielded also higher 1-butene conversion with increasing 1-butene feed concentration, while the activity of the catalyst with 7 nm deposited particles steadily decreased after 44 h time on stream. This suggests that the 1 × Si 7 catalyst deactivated gradually over time possibly due to the formation and accumulation of aldol condensation products in the pore structure [21, 33]. In line with this, the selectivity of aldol condensation products remained negligible in the 1 × Si 70 and 2 × Si 70 supported catalysts (ca. 1%) during all 140 h time on stream, while the 1 × Si 7 catalyst showed higher aldol formation throughout the catalytic run (Fig. 7a). The 2 × Si 70-calc. catalyst with intermediate calcination between deposition of each SiO_2 washcoat layer formed also only aldol condensations products during the first 60 h time on stream. The higher aldol selectivity of the 2 × Si 70-calc. support compared to the 2 × Si 70 can potentially be due to the changes in the distribution of silica NPs such as e.g., formation of more dead-end pores caused by the intermittent

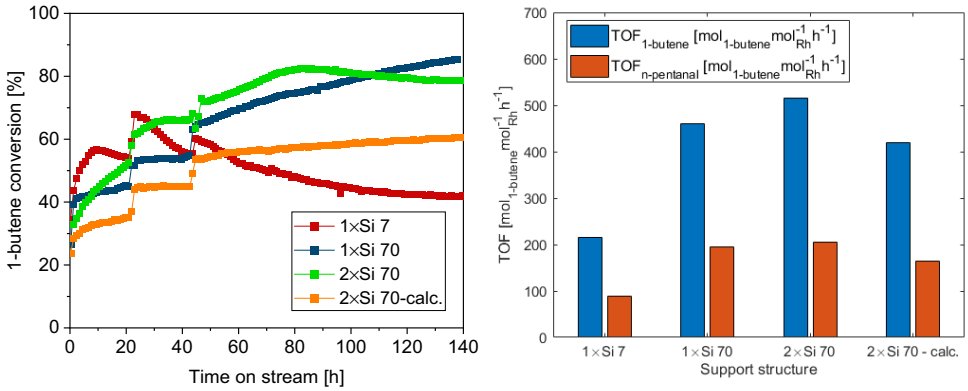

Fig. 6 Conversion of 1-butene (left) and TOF of 1-butene and n-pentanal (TOS = 44–140 h) in semi-steady state (right) from 1-butene HyFo with 1 × Si 7, 1 × Si 70, 2 × Si 70, and 2 × Si 70-calc. SiC monoliths with Rh-bpp-sebacate SLP catalyst system. Reaction conditions: T = 120 °C, p_{feed} = 10 bar, Rh/bpp/sebacate molar ratio = 1/4/16, Rh-loading = 12.70, 12.05, 10.11, and 9.74 mg in 1 × Si 7, 1 × Si 70, 2 × Si 70, and 2 × Si 70-calc. supports, respectively. Flow rates of carbon monoxide, hydrogen, 1-butene, and nitrogen feed as reported in Table 2

calcination. Dead-end pores can likely prolong the residence time of aldehydes and hence potentially causing more aldol formation. However, as the 2 × Si 70-calc. support exhibited both less favorable aldol selectivity and was more expensive and energy-consuming to produce, the practical usefulness of these results should be stressed, and intermediate calcinations will be avoided in the future.

Thermogravimetric analysis on 1 × Si 7 and 1 × Si 70 samples was conducted after reaction to observe if aldol condensation products were retained inside the porous network. The results did not reveal weight losses higher than expected due to the catalyst phase, thus not confirming the presence of aldols inside the pores. This, however, does not rule out the presence of condensed aldols in 1 × Si 7 and 1 × Si 70 as the samples underwent post reaction treatment at 120 °C and 1 bar in a stream of nitrogen for several hours.

Schörner et al. [36] have previously demonstrated that the accumulation of aldehydes and the subsequent formation of aldol condensation products in 1-butene HyFo increase with decreasing median mesopore sizes in support materials. Therefore, the higher selectivity of aldol condensation products in the 1 × Si 7 supported catalyst might be due to the small sized mesopores in this catalyst. The varying amount of mesopore volume has profound effects on the character of the liquid catalyst phase as expressed by the mesopore filling degree (δ) (Table 3, see Eqs. S5–S7 in the supporting information for detailed calculations) and film thickness (Table S1; obtained according to Eq. S8). The supports containing 70 nm NPs do not only have wider mesopores but also lower pore filling degrees. Hence, once formed, aldehydes are likely to escape into macropores, avoiding aldol formation. In the 1 × Si 7 system, on the other hand, the mesopores are prone to be practically filled with liquid phase (Fig. 5). As a result, the gas–liquid interface is here probably confined to the pore necks, which can hamper release of aldehydes from the liquid phase thus promoting aldol formation.

The selectivity of n-pentanal and the linear to total (linear + branched) aldehydes ratio obtained for the SLP catalysts are shown in Figs. 7c and d, respectively. The SLP catalysts with one layer of 7 and 70 nm SiO_2 washcoats showed marginally higher selectivities for linear pentanal (ca. 40–45%), while the highest and most stable linear to total aldehyde ratio was clearly obtained for the SLP catalyst with 1 × Si 7 support (ca. 98–99%). Hence, the increased aldol formation for this catalyst had apparently no negative effect on the linear to total aldehyde selectivity. The 2-butene selectivity at TOS = 60–140 h (Fig. 7b) was also lower in the 1 × Si 7 and 1 × Si 70 supported catalysts compared to the 2 × Si 70 and 2 × Si 70-calc. systems, thus enhancing the selectivity of the corresponding materials towards n-pentanal.

The theoretically calculated pore filling degree was investigated to understand the selectivity and activity results in more detail for each SLP catalyst. According to Pelt et al. [37], the degree of pore filling of SLP catalysts influences both activity and the n/iso aldehyde selectivity in the gas-phase HyFo reaction, because two types of Rh-complexes with different ligand coordination sphere are predominantly present in the systems at the gas–liquid interface and the bulk liquid depending on the availability of the ligands. At the gas–liquid interface are CO coordinated Rh-complexes preferentially formed, since the concentration of CO gas is higher than in bulk liquid, and a higher fraction of such complexes leads to lower n/iso aldehyde selectivity but higher catalytic activity. In addition, with a relatively low pore filling degree the surface area to volume ratio of the gas–liquid interface significantly increases [38], as also seen in the MIP

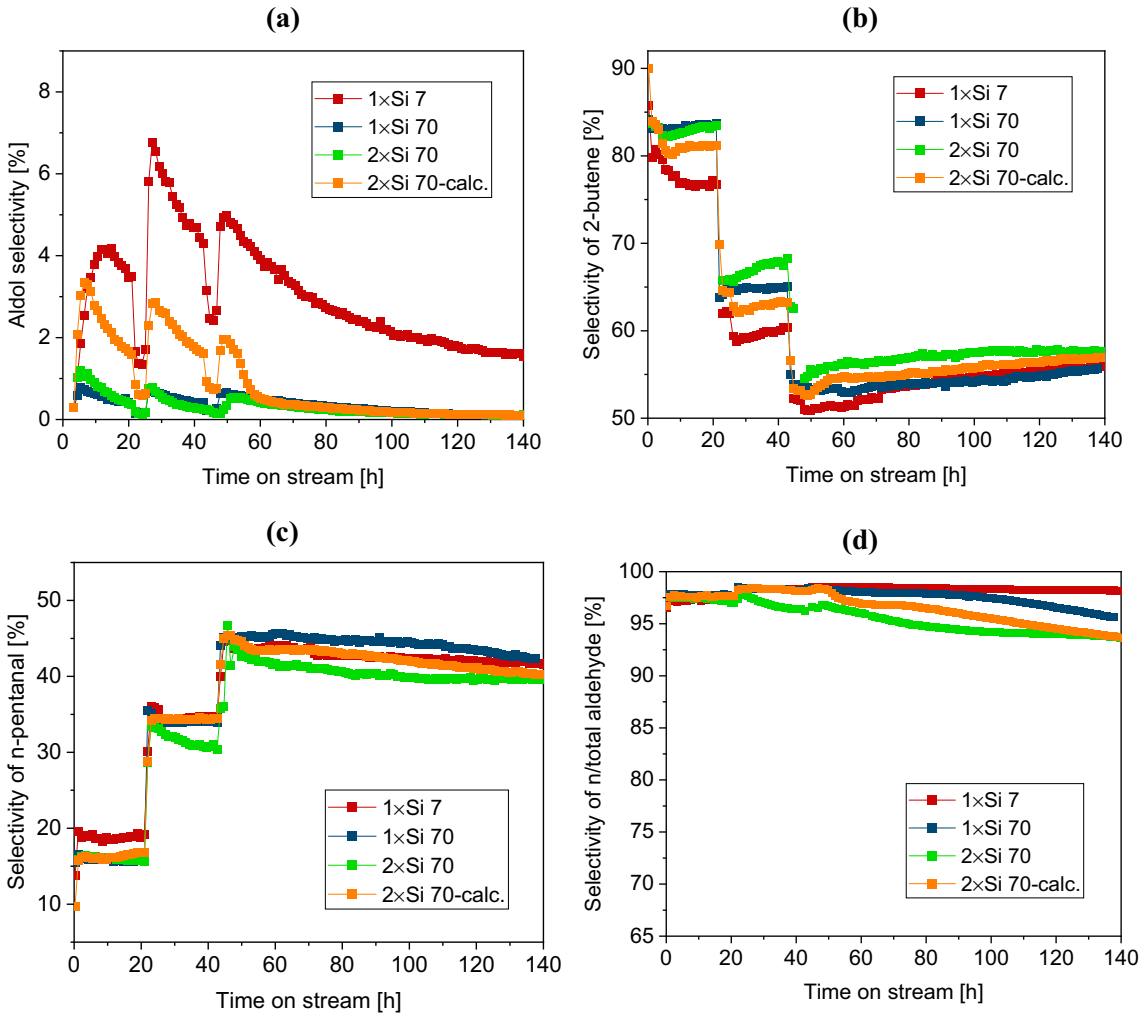

Fig. 7 Selectivity of **a** aldol condensation products, **b** 2-butene, **c** n-pentanal, and **d** linear to total aldehyde ratio in HyFo of 1-butene with 1×Si 7, 1×Si 70, 2×Si 70, and 2×Si 70-calc. SiC monoliths impregnated by Rh-bpp-sebacate SLP catalyst system. Reaction conditions: T = 120 °C, p_{feed} = 10 bar, Rh/bpp/sebacate molar ratio = 1/4/16, Rh-loading = 12.70, 12.05, 10.11, and 9.74 mg in 1×Si 7, 1×Si 70, 2×Si 70, and 2×Si 70-calc. supports, respectively. The flow rates of carbon monoxide, hydrogen, 1-butene, and nitrogen feed as reported in Table 2

Table 3 Theoretically calculated mesopore volume of silica washcoats for different supports and corresponding pore filling degree of each support by the catalyst stock solution after impregnation

Monolithic support	Content of SiO_2 (g)	Mesopore volume of SiO_2 (mL)	Pore filling degree, δ (%)[a]
1×Si 7	7.4	1.3	104
1×Si 70	9.5	2.0	77
2×Si 70	15.7	2.7	39
2×Si 70-calc	17.5	3.0	33

[a]Calculated as: $100 \times V_{liquid} \times V_{mesopore}^{-1}$

results of this work. Hence, a low pore filling degree will also contribute to decrease the n/iso aldehyde selectivity and increase catalytic activity. The catalytic performance observed for the different Rh-bpp-sebacate SLP catalyst systems is in line with the rationalization by Pelt et al. as the δ value was relatively high, when less SiO_2 was loaded into the SiC monoliths (Table 3). Hence, with low pore filling degree the thickness of the catalytic film will be lower and the liquid will be exposed to more CO molecules resulting in less bpp coordination, and finally lower selectivity towards n-pentanal.

Moreover, referring to the BET analysis of the 1×Si 7 support (Fig. 5) the volume created by pores smaller than 15 nm, ca. 0.015 mL g^{-1}, roughly matched the volume of liquid phase (0.013 mL g^{-1}), corroborating the mesopore filling

degree as calculated by Eq. S7. As most of the mesopores are likely completely filled with liquid, Eq. S8 cannot be used for the film thickness calculation for the 1 × Si 7 support, and the liquid–gas interface area is thus limited to the pore openings. The pore opening area of a mesopore is expected to be significantly lower than the surface area inside the pore as long as the pore lengths is significantly higher than the pore diameter. Hence, it is reasonable to assume that the gas–liquid interface was significantly smaller in the 1 × Si 7 support than in the other supports, and accordingly the hypothesis by Pelt et al. can potentially explain the high and stable regioselectivity observed for the 1 × Si 7 catalyst system.

Based on both experimental CO solubility measurements as well as COSMOthermX19 calculations, Schörner et al. [39] reported that the activity of sebacate-based SLP HyFo catalysts are likely limited by low solubility of syngas at temperatures higher than 110 °C. Moreover, when the group conducted kinetic measurements on a SLP catalyst system comprising a 1 × Si 7-like support and the liquid phase composition as used in the current study, but with a liquid loading about four times higher (0.05 vs. 0.012 wt.% Rh), CO reaction orders for n-pentanal (0.8) and 2-methylbutanal (0.9) were found to not differ significantly. The very high pore filling degree used in the latter system made it even more bulk-like than in the herein reported 1 × Si 7 system, and the limited CO solubility in bulk sebacate probably restricted formation of CO coordinated complexes. Hence, a high liquid–gas interface area as found in the catalysts with low mesopore filling degree seems to be required for this to occur.

Autocatalytic ligand deterioration [40] is another possible cause of the declining regioselectivity of the SLP catalysts based on 1 × Si 7, 1 × Si 70, and 2 × Si 70-calc. supports if silanol groups participate in the hydrolysis of bpp ligand and form phosphorous acid, which catalyzes the ligand decomposition [41]. ^{29}Si solid-state MAS NMR was therefore used to quantify the relative abundance of geminal silanols (Q2), vicinal silanols (Q3) and siloxane groups (Q4) and calculate the molar OH/Si ratios in the 1 × Si 7, 1 × Si 70 and 2 × Si 70-calc. supports, respectively (Fig. S12 and Table S2). The lower Si/bpp, and more importantly, lower OH/bpp molar ratio could potentially contribute to the more stable regioselectivity observed for the 1 × Si 7 based catalyst. However, also this system should suffer from declining regioselectivity in longer term testing if silanol-initiated autocatalytic ligand decomposition takes place. To verify the proposed reasons of deactivation follow up experiments are planned to be completed in the near future, including variation of support calcination temperatures which could alter the number of silanol groups and hence improve the regioselectivity performance of the resulting catalysts.

Lastly, the catalytic performance of the 1 × Si 70 SLP catalyst was compared to similar catalysts in literature for 1-butene HyFo (Table S3). One should pay attention to the differences in applied temperatures and 1-butene inlet concentrations in each study as lower reaction temperature slows down isomerization and improves n/total aldehyde selectivity, while higher concentrations of 1-butene positively influences the activity in terms of TOF. Compared to the similar catalysts found in literature, the 1 × Si 70 SLP catalyst showed at higher reaction temperature (120 °C) more isomerization to 2-butene and lower n-aldehyde selectivity, but negligible formation of aldol condensation products as well as high activity despite using a highly diluted 1-butene feed. Importantly, the SLP catalyst system also proved long-term stability (140 h time on stream) making it attractive for industrial use.

4 Conclusions

SLP catalysts comprised of monolithic SiC support materials impregnated with Rh-bpp-sebacate have shown promising catalytic performance in continuous gas-phase HyFo of 1-butene. To investigate the influence of the support structure in the SLP catalyst systems, the textural properties of the SiC monoliths were modified with SiO_2 NPs with different sizes in different loadings, and with intermediate calcination of the SiO_2 washcoat. Deposition of SiO_2 NPs into the SiC supports led to the formation of new intraparticle mesopores, expected to be beneficial for the SLP systems to retain the liquid catalyst phase by reinforcement of the capillary forces.

The prepared SLP systems demonstrated long-term stability of the catalysts in the gas-phase HyFo of 1-butene, i.e. during 140 h time on stream, with negligible formation of high boilers for the 1 × Si 70 and 2 × Si 70 supported catalysts. The lower formation and accumulation of the aldol condensation products was attributed to the high pore area of these supports compared to the corresponding 7 nm SiO_2 loaded catalysts. The two catalysts presented also the highest catalytic activity comprising 1-butene conversion of ca. 80% corresponding to n-pentanal TOF of ca. 500 $mol_{1\text{-butene}}\ mol_{Rh}^{-1}\ h^{-1}$. The support structure also influenced the catalyst selectivity towards linear pentanal by affecting the degree of pore filling of the SLP catalysts. The results showed that the catalytic activity was higher for the SLP catalysts with a low degree of pore filling, which could be attributed to preferential formation of catalytically active Rh-complexes at the gas–liquid interface having lower bpp coordinated. In line with this, the catalysts were also less regioselective towards n-pentanal. Overall, the prepared SLP systems showed attractive catalytic performance but further optimization of, e.g. catalyst components and liquid loading, is needed to make the technology prone for industrial implementation.

Supplementary Information The online version contains supplementary material available at https://doi.org/10.1007/s11244-023-01792-w.

Acknowledgements The authors gratefully acknowledge financial support from the European Commission within the Horizon2020-SPIRE project MACBETH under grant agreement N°869896. The authors would also like to thank Ping Zhu (Technical University of Denmark) for SEM analysis and Kasper Enemark-Rasmussen (Technical University of Denmark) for performing ^{29}Si solid-state MAS NMR.

Funding Horizon 2020, 869896

Declarations

Conflict of interest There are no conflicts to declare.

References

1. Jess A, Wasserscheid P (2013) Chemical Technology. An Integral Textbook. Wiley Online Library
2. van Leeuwen PWNM (2004) Catalysis, homogeneuos. Understanding the Art. Kluwer Academic Publishers, Dordrecht
3. Behr A, Neubert P (2012) Applied homogeneous catalysis. Wiley, Newyork
4. Bailar JC Jr (1974) "Heterogenizing" homogeneous catalysts. Catal Rev: Sci Eng 10(1):17–36
5. Fehrmann R, Riisager A, Haumann M (2014) Supported ionic liquids: fundamentals and applications. Wiley, New York
6. Marinkovic JM, Riisager A, Franke R, Wasserscheid P, Haumann M (2018) Fifteen years of supported ionic liquid phase-catalyzed hydroformylation: material and process developments. Ind Eng Chem Res 58(7):2409–2420
7. Riisager A, Fehrmann R, Haumann M, Wasserscheid P (2006) Supported ionic liquid phase (SILP) catalysis: An innovative concept for homogeneous catalysis in continuous fixed-bed reactors. Eur J Inorg Chem 4:695–706
8. Moravec RZ, Schelling WT, Oldershaw CF (1939) British Patent 511,566. In: Chem Abstr (1940) 43:7102
9. Moravec RZ, Schelling WT, Oldershaw CF (1941) Canadian Patent 396,994. In: Chem Abstr (1941) 35:6103
10. Ciapetta FG U.S. Patent (1947) 2,430,803. In: Chem Abstr (1948) 42:1398
11. Riisager A, Fehrmann R, Flicker S, van Hal R, Haumann M, Wasserscheid P (2005) Very stable and highly regioselective supported ionic-liquid-phase (SILP) catalysis: continuous-flow fixed-bed hydroformylation of propene. Angew Chem Int Ed 44(5):815–819
12. Riisager A, Eriksen KM, Wasserscheid P, Fehrmann R (2003) Propene and 1-octene hydroformylation with silica-supported, ionic liquid-phase (SILP) Rh-phosphine catalysts in continuous fixed-bed mode. Catal Lett 90(3):149–153
13. Riisager A, Wasserscheid P, van Hal R, Fehrmann R (2003) Continuous fixed-bed gas-phase hydroformylation using supported ionic liquid-phase (SILP) Rh catalysts. J Catal 219(2):452–455
14. Rogers RD, Seddon KR (2005) Ionic liquids IIIB: fundamentals progress challenges and opportunities: transformations and processes. ACS Publications, Washington
15. Mehnert CP, Cook RA, Dispenziere NC, Afeworki M (2002) Supported ionic liquid catalysis– A new concept for homogeneous hydroformylation catalysis. J Am Chem Soc 124(44):12932–12933
16. Mehnert CP (2005) Supported ionic liquid catalysis. Chem Eur J 11(1):50–56
17. Franke R, Selent D, Börner A (2012) Applied hydroformylation. Chem Rev 112(11):5675–5732
18. Cunillera A, Godard C, Ruiz A (2017) Asymmetric hydroformylation using rhodium. Rhodium Catal. https://doi.org/10.1007/3418_2017_176
19. Riisager A, Fehrmann R, Haumann M, Gorle BS, Wasserscheid P (2005) Stability and kinetic studies of supported ionic liquid phase catalysts for hydroformylation of propene. Ind Eng Chem Res 44(26):9853–9859
20. Franke R, Hahn H (2015) A catalyst that goes to its limits. Evonik Ind 2:18–23
21. Kaftan A, Schönweiz A, Nikiforidis I, Hieringer W, Dyballa KM, Franke R, Görling A, Libuda J, Wasserscheid P, Laurin M (2015) Supported homogeneous catalyst makes its own liquid phase. J Catal 321:32–38
22. Logemann M, Marinkovic JM, Schörner M, García-Suárez EJ, Hecht C, Franke R, Wessling M, Riisager A, Fehrmann R, Haumann M (2020) Continuous gas-phase hydroformylation of but-1-ene in a membrane reactor by supported liquid-phase (SLP) catalysis. Green Chem 22(17):5691–5700
23. Portela R, Marinkovic JM, Logemann M, Schörner M, Zahrtman N, Eray E, Haumann M, García-Suárez EJ, Wessling M, Ávila P, Riisager A, Fehrmann F (2022) Monolithic SiC supports with tailored hierarchical porosity for molecularly selective membranes and supported liquid-phase catalysis. Catal Today 383:44–54
24. Jakuttis M, Schönweiz A, Werner S, Franke R, Wiese KD, Haumann M, Wasserscheid P (2011) Rhodium-Phosphite SILP Catalysis for the Highly Selective Hydroformylation of Mixed C4 Feedstocks. Angew Chem 123(19):4584–4588
25. Herman J, van den Berg P, Scholten J (1987) The industrial hydroformylation of olefins with a rhodium-based supported liquid phase catalyst (SLPC): IV: Heat-transfer measurements in a fixed bed containing alumina SCS9 particles. Chem Eng J 34(3):133–142
26. Rase HF, Holmes JR (1977) Chemical reactor design for process plants, vol 2. Wiley, New York
27. Ledoux MJ, Pham-Huu C (2001) Silicon carbide: a novel catalyst support for heterogeneous catalysis. CATTECH 5(4):226–246
28. Reay D, Ramshaw C, Harvey A (2013) Process intensification: engineering for efficiency, sustainability and flexibility. Butterworth-Heinemann
29. Marinkovic JM (2019) Supported Ionic Liquid-Phase (SILP) membrane reaction systems for industrial homogeneous catalysis. Technical University of Denmark, Denmark
30. Stobbe P (2010) Porous ceramic body and method for production thereof, U.S. Patent 7,699,903
31. Jørgensen JH (2021) A method of producing a ceramic support and a ceramic support. WO2021116410:A2
32. Washburn EW (1921) The dynamics of capillary flow. Phys Rev 17(3):273

33. Schönweiz A, Debuschewitz J, Walter S, Wölfel R, Hahn H, Dyballa KM, Franke R, Haumann M, Wasserscheid P (2013) Ligand-modified rhodium catalysts on porous silica in the continuous gas-phase hydroformylation of short-chain alkenes–catalytic reaction in liquid-supported aldol products. ChemCatChem 5(10):2955–2963
34. Portela R, Wolf P, Marinkovic JM, Serrano-Lotina A, Riisager A, Haumann M (2021) Tailored monolith supports for improved ultra-low temperature water-gas shift reaction. React Chem Eng 6(11):2114–2124
35. Marinkovic JM, Benders S, Garcia-Suarez EJ, Weiß A, Gundlach C, Haumann M, Küppers M, Blümich B, Fehrmann R, Riisager A (2020) Elucidating the ionic liquid distribution in monolithic SILP hydroformylation catalysts by magnetic resonance imaging. RSC Adv 10(31):18487–18495
36. Schörner M, Rothgängel P, Mitländer K, Wisser D, Thommes M, Haumann M (2021) Gas-Phase Hydroformylation Using Supported Ionic Liquid Phase (SILP) Catalysts-Influence of Support Texture on Effective Kinetics. ChemCatChem 13(19):4192–4200
37. Pelt H, De Munck N, Verburg R, Brockhus J, Scholten J (1985) Hydroformylation of butene-1 and butene-2 over rhodium-slp catalysts, as compared with the hydroformylation of ethene and propene: Part III. The influence of the degree of pore-filling on the performance. J Mol Catal 31(3):371–383
38. Pelt H, Brockhus J, Verburg R, Scholten J (1985) Hydroformylation of alkenes with supported liquidphase rhodium catalysts: the influence of the dissolution of the produced alkanals on catalytic performance. J Mol Catal 31(1):107–118
39. Schörner M, Mitländer K, Wolf M, Franke R, Haumann M (2022) Silicon carbide supported liquid phase (SLP) hydroformylation catalysis-effective reaction kinetics from continuous gas-phase operation. ChemCatChem 14(12):e202200058
40. Kloß S (2020) Influence of the Ligand structure on the hydroformylation of olefins. Universität Rostock, Rostock
41. McIntyre SK, Alam TM (2007) ^{17}O NMR investigation of phosphite hydrolysis mechanisms. Magn Reson Chem 45(12):1022–1026